

Sound transmission through a periodic cascade with application to drill pipes

Niels J. C. Lous, Sjoerd W. Rienstra, and Ivo J. B. F. Adan

Eindhoven University of Technology, P.O. Box 513, 5600 MB Eindhoven, The Netherlands

(Received 21 March 1997; revised 8 January 1998; accepted 16 January 1998)

Acoustical data transmission through the wall of drill pipes is considered. Drill pipes are known to behave like bandpass filters; the position of the pass bands can be determined analytically. This work extends the frequency domain drill pipe models presented by Barnes and Kirkwood [*J. Acoust. Soc. Am.* **51**, 1606–1608 (1972)], and more recently by Drumheller [*J. Acoust. Soc. Am.* **85**, 1048–1064 (1989)]. The approach discussed in this paper has the advantage that it yields explicit expressions for the fine structure of the drill pipe's frequency response in the pass bands. It furthermore allows the effect of energy dissipation and pipe segment length variations to be included in the model. The emphasis of the paper, however, lies on the time domain modeling of the drill pipe. The propagation of sound energy pulses through its wall, and the effect of multiple reflections and/or transmissions during this propagation, are described using a Markov chain. Explicit expressions result for the expected duration of an energy pulse's trip from one end of the drill pipe to the other, depending upon the number of drill pipe segments and the transmission coefficient at the tool-joints connecting them. The results are applicable to any situation where sound or energy transmission through a cascade of acoustic components occurs. © 1998 *Acoustical Society of America*. [S0001-4966(98)00705-X]

PACS numbers: 43.20.Mv, 43.20.Tb, 43.40.Ph [JEG]

INTRODUCTION

When performing soil drillings, one needs to know on the platform what happens at the drill bit. Adverse soil conditions and a too high temperature, among others, may invoke the necessity to stop drilling in order to avoid material damage. Relevant information may be gathered by equipment installed in the drill bit, but conveying the measured data to the platform is a problem as the severe circumstances in the bore hole do not allow wires to be installed.

The only communication method between drill bit and platform applied in practice is modulation of the mud stream inside the drill pipe. This stream is pumped downward through the pipe to cool or to drive the bit. At the lower pipe end, the drill pipe can be closed or opened by means of a flap. Closing the flap causes the pressure in the mud stream to increase, which can be measured at the upper drill pipe end. One information bit thus can be conveyed by respectively closing and opening the flap during one time unit. This method allows only a few bits to be transmitted each second.

In the present study, an alternative is considered where acoustical data are transmitted through the drill pipe wall (see also Barnes and Kirkwood, 1972; Drumheller, 1989). The drill pipe, consisting of steel, hollow, cylindrical segments, each about 10 m long, is excited at the lower end by a piezoelectrical transducer or by a hammer. The resulting sound signals travel through the wall of these segments, but are partly reflected at the tool-joints connecting them. Depending upon the reflection and transmission properties of the tool-joints, where the wall is thicker and includes a screw thread, sound signals of given frequencies do or do not reach the upper drill pipe end, with or without distortion and delay.

We first briefly discuss our drill pipe model in the frequency domain, which is similar to the one in Drumheller

(1989), but allows a further-going analytical description of the data transmission process. We list the main modeling assumptions, give a short description of the behavior of tool-joints and pipe segments, and come to equations representing the transmission properties of the whole drill pipe. We then apply our model to consider energy dissipation and pipe segment length variations.

In the time domain, we introduce a few more modeling assumptions, and describe the configuration in terms of a Markov chain. This yields expressions for the time energy (or sound) pulses need to travel through the pipe.

We refer to Fig. 1 for names of drill pipe parts.

Both the frequency domain analysis and the time domain expressions are applicable to any situation where sound or energy transmission through a cascade of acoustic components occurs. In speech production models, for instance, the vocal tract shape is usually approximated by a series of small cylindrical tubes, not unlike a drill pipe. One of the main contributions of this paper is that we derive explicit expressions for the transmission behavior of a cascade of (regular) acoustic components. The emphasis, however, lies on the Markov chain analogue to the drill pipe, which extends the frequency domain results (Drumheller, 1989; Barnes and Kirkwood, 1972) to the time domain.

I. MODELING ASSUMPTIONS AND THEIR MOTIVATION

In this section, we introduce and motivate a number of modeling assumptions to obtain a mathematical description of the drill pipe.

We assume the whole configuration to be "ideal" in the sense that all pipe segments and tool-joints are exactly cylin-

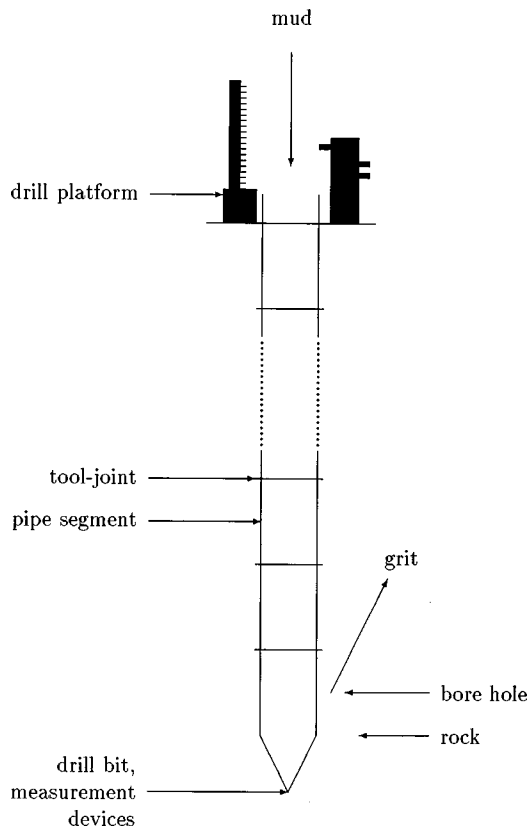


FIG. 1. Drill pipe.

dricial, with a homogeneous wall of constant thickness, and that the screw thread of one tool-joint fits precisely into that of the next.

When the drill pipe is excited at its lower end, longitudinal, transversal, and spiraling sound waves result. The latter two cause wall displacements perpendicular to the pipe axis, and thus interact with the environment. As a consequence, they lose part of their energy by radiation. Furthermore, for the low frequencies considered (see below), any spiraling modes are cut off and will eventually vanish. Longitudinal waves, corresponding to wall displacements parallel to the pipe axis, are therefore likely to prevail in long drill pipes. In the sequel, we restrict ourselves to longitudinal sound waves. The cylindrical symmetry of the configuration implies that a one-dimensional mathematical description suffices.

We choose the co-ordinate system such that the z axis corresponds to the drill pipe axis (see Fig. 2). In drill pipe

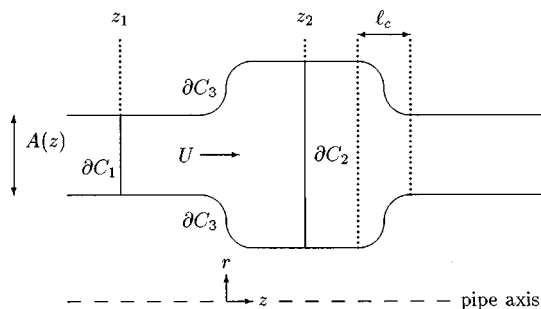


FIG. 2. Drill pipe wall of variable surface.

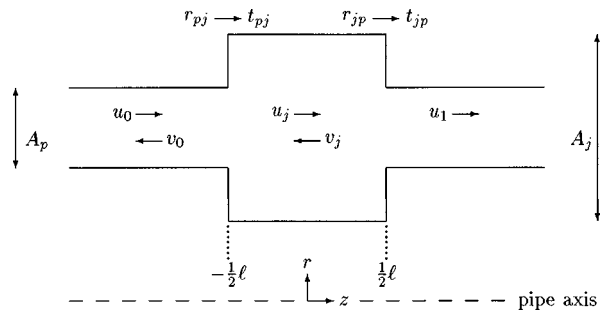


FIG. 3. Tool-joint modeled for large wave lengths.

parts where the configuration wall surface is constant, a combination of Newton's and Hooke's laws (Timoshenko *et al.*, 1974) yields an ordinary one-dimensional wave equation for the longitudinal displacement $U(z, t)$,

$$\frac{\partial^2 U}{\partial t^2} - c^2 \frac{\partial^2 U}{\partial z^2} = 0. \quad (1)$$

Its harmonic solutions are combinations of sound waves traveling to the left and to the right,

$$U(z, t) = \{u e^{i\kappa z} + v e^{-i\kappa z}\} e^{-i\omega t}, \quad (2)$$

in which $\kappa = \omega/c$ is the ratio of angular frequency and speed of sound in steel.

To simplify the model, we neglect the (cutoff) higher-order modes, and assume the plane waves (2) to be stepwise discontinuously connected at the joints. This assumption is reasonable for frequencies at which the wavelength λ is sufficiently larger than the drill pipe wall thicknesses h_p in the pipe segments, and h_j in the tool-joints. The length ℓ_c of the curved tool-joint part should typically not be much larger than h_p or h_j . Furthermore, to avoid tunneling effects, both the pipe segment length L and the tool-joint length ℓ should exceed the geometrical parameters h_p , h_j , and ℓ_c at the curved tool-joint parts. For the considered drill pipe, $h_p = 1$ cm, $h_j = 3.5$ cm, $\ell_c = 5$ cm, $L = 9.1$ m, and $\ell = 0.5$ m. The model is therefore restricted to frequencies satisfying $f \ll c/\ell_c \approx 100$ kHz for $c = 5100$ m/s in steel. Results are presented for frequencies up to 10 kHz.

We thus have reduced the real configuration to a series of straight segments and tool-joints in which only longitudinal, harmonic sound waves propagate. The drill pipe is driven at the lower end by a transducer; the upper end is assumed to reflect all sound waves completely, which follows from the observation that the normal force at that end equals zero, and Hooke's law.

We proceed by capturing tool-joints, transducer, and pipe segments in mathematical expressions. Their combination will yield the mathematical model.

II. FREQUENCY DOMAIN MODELING

In the sequel, we consider a drill pipe configuration consisting of $N + 1$ pipe segments, numbered $n = 0, \dots, N$, and N tool-joints, numbered $n = 1, \dots, N$ (see Fig. 4). The outer ends may be counted as "tool-joints" 0 and $N + 1$. The length of the n th pipe segments is L_n .

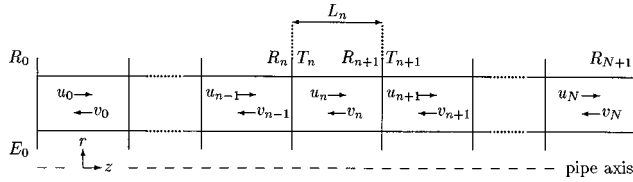


FIG. 4. Drill pipe modeled using reflection and transmission coefficients.

A. A tool-joint, transducer, and pipe segment model

We first describe a tool-joint in terms of reflection and transmission coefficients $R = v_0/u_0$ and $T = u_1/u_0$ (see Fig. 3) (Dowling and Ffowcs Williams, 1983, pp. 66–67).

We choose the origin of the coordinate system to correspond with the middle of a tool-joint with length ℓ . Continuity of displacement and normal force implies that at $z = -\frac{1}{2}\ell$, $U_0 = U_j$, and $A_p \partial U_0 / \partial z = A_j \partial U_j / \partial z$; A_p and A_j denote the wall surface of pipe segment and tool-joint, respectively. Similar equations result at $z = \frac{1}{2}\ell$. Substitution of (2)—with the correct wave amplitudes—into these expressions yields

$$R = 2i \frac{r_{pj} \sin(\kappa \ell)}{1 - r_{jp}^2 \vartheta^4} \quad \text{and} \quad T = \frac{t_{pj} t_{jp}}{1 - r_{jp}^2 \vartheta^4}, \quad (3)$$

where $\vartheta = e^{i\kappa \ell/2}$. The coefficients $r_{jp} = (A_j - A_p)/(A_j + A_p)$, $t_{jp} = 1 - r_{jp}$, $r_{pj} = -r_{jp}$, and $t_{pj} = 1 - r_{pj}$ describe sound reflection at each of the wall area discontinuities¹ (Dowling and Ffowcs Williams, 1983, p. 64; Fletcher and Rossing, 1991, pp. 147–148).

Denoting the displacement amplitude in the pipe segment to which the transducer is connected by U_0 , and assuming U_0 to satisfy (2), a mathematical model of a transducer (van de Ven, 1975) yields

$$u_0 = \phi_0 E_0 + \phi_0^2 R_0 v_0, \quad (4)$$

where R_0 and E_0 are two transducer-dependent constants, and $\phi_0 = e^{i\kappa L_0/2}$ is a phase change. The factor R_0 is similar to a reflection coefficient, but the transducer also keeps feeding energy into the drill pipe, which is described by the factor E_0 .

If we substitute $z + \Delta z$ for z in Eq. (2), it appears that for sound waves that travel a distance Δz , only the phase changes by a factor $e^{i\kappa \Delta z}$. As a consequence, the pipe segments can be modeled as phase shifts.² We introduce the factor $\phi_n = e^{i\kappa L_n/2}$, describing the phase change of a sound wave traveling through half of the pipe segment n , i.e., over a distance $\frac{1}{2}L_n$.

B. A segmented drill pipe model

We denote the amplitude of the sound wave traveling to the right in the middle of pipe segment n by u_n ; the wave moving to the left at that location has amplitude v_n . The reflection and transmission coefficients at tool-joint n are denoted R_n and T_n . We choose $z=0$ in the middle of the pipe segment connected to the transducer. We find

$$u_n = \phi_{n-1} T_n \phi_n u_{n-1} + \phi_n R_n \phi_n v_n, \quad n = 1, \dots, N,$$

$$v_n = \phi_{n+1} T_{n+1} \phi_n v_{n+1} + \phi_n R_{n+1} \phi_n u_n,$$

$$n = 0, \dots, N-1,$$

or, after rewriting in terms of matrices and applying induction,

$$\begin{pmatrix} u_N \\ v_N \end{pmatrix} = \left(\prod_{n=1}^N (\Phi_n M_n \Phi_{n-1}) \right) \begin{pmatrix} u_0 \\ v_0 \end{pmatrix} =: \mathcal{T} \begin{pmatrix} u_0 \\ v_0 \end{pmatrix}, \quad (5)$$

with

$$\Phi_n = \begin{pmatrix} \phi_n & 0 \\ 0 & \phi_n^{-1} \end{pmatrix} \quad \text{for } n = 0, \dots, N, \quad (6)$$

and

$$M_n = \begin{pmatrix} (T_n^2 - R_n^2)/T_n & R_n/T_n \\ -R_n/T_n & 1/T_n \end{pmatrix} \quad \text{for } n = 1, \dots, N. \quad (7)$$

The phase-shift matrices Φ_n and Φ_{n-1} describe the propagation of sound waves through (half) pipe segments; M_n models sound reflection and transmission at the joint between segments $n-1$ and n . \mathcal{T} describes the behavior of sound waves traveling from segment 0 to segment N , and \mathcal{T}^{-1} how sound waves propagate in the opposite direction. Symmetry thus implies that $\det(\mathcal{T}) = \det(\mathcal{T}^{-1})$, and therefore $\det(\mathcal{T}) = 1$.

Assuming all pipe segments to have the same length L , and all tool-joints to have identical properties ℓ , ϕ , R , T , and M , we have $\mathcal{T} = (\Phi M \Phi)^N =: \mathcal{M}^N$. The powers of \mathcal{M} can be determined explicitly, allowing explicit analytical results for the case $N \rightarrow \infty$.

The Cayley–Hamilton theorem (Tropper, 1969, pp. 72–73) states that each square matrix satisfies its characteristic equation, so that $\mathcal{M}^2 - 2\tau \mathcal{M} + \mathcal{I} = 0$, where

$$\tau = \frac{1}{2} \text{tr}(\mathcal{M}) = \frac{1}{2} (\mathcal{M}_{11} + \mathcal{M}_{22}),$$

and we used the fact that the determinant of \mathcal{M} is given by $\det \mathcal{M} = \mathcal{M}_{11} \mathcal{M}_{22} - \mathcal{M}_{12} \mathcal{M}_{21} = \det(\Phi) \det(M) \det(\Phi) = 1 \cdot 1 \cdot 1 = 1$. The characteristic equation implies that \mathcal{M}^n must be a linear combination of \mathcal{M} and the unity matrix \mathcal{I} , i.e., $\mathcal{M}^n = a_n \mathcal{M} + b_n \mathcal{I}$. Similarly, the eigenvalues $\lambda_{1,2}$ of \mathcal{M} satisfy its characteristic equation, and therefore $\lambda_{1,2}^n = a_n \lambda_{1,2} + b_n$. Some straightforward computations give

$$\lambda_{1,2} = \tau \pm \sqrt{\tau^2 - 1}, \quad \text{while } \lambda_1 \lambda_2 = 1.$$

Combination of the latter two expressions yields two equations for a_n and b_n , from which both coefficients can be determined (assuming $\tau^2 \neq 1$, so that $\lambda_1 \neq \lambda_2$). This yields the following expressions for the coefficients of \mathcal{M}^N :

$$\mathcal{M}_{11}^N = \frac{1}{\lambda_1 - \lambda_2} \{ (\mathcal{M}_{11} - \lambda_2) \lambda_1^N - (\mathcal{M}_{11} - \lambda_1) \lambda_2^N \}, \quad (8)$$

$$\mathcal{M}_{12}^N = \frac{1}{\lambda_1 - \lambda_2} \{ \mathcal{M}_{12} \lambda_1^N - \mathcal{M}_{12} \lambda_2^N \} = -\mathcal{M}_{21}^N, \quad (9)$$

$$\mathcal{M}_{22}^N = \frac{1}{\lambda_1 - \lambda_2} \{ (\mathcal{M}_{22} - \lambda_2) \lambda_1^N - (\mathcal{M}_{22} - \lambda_1) \lambda_2^N \}. \quad (10)$$

If $\tau^2 = 1$, similar expressions for the components of \mathcal{M}^N can be found by taking limits for τ tending to ± 1 in the latter equations.

At the platform end of the drill pipe, we have

$$v_N = \phi_N^2 R_{N+1} u_N. \quad (11)$$

Since all pipe segments are assumed to have the same length, $\phi_N = \phi$. Furthermore, in all numerical calculations performed in the sequel, we set $R_{N+1} = 1$, which corresponds to total reflection at the platform end of the configuration.

We thus have derived the four linear equations (4), (5), and (11) for the unknown amplitudes u_0 , v_0 , u_N , and v_N . Some calculations yield the total amplitude $U_N = u_N + v_N$ of the sound wave in the middle of pipe segment N :

$$U_N = \frac{\phi E_0 (1 + \phi^2 R_{N+1}) \mathcal{M}_{11}^N}{1 - (\phi^2 R_0 \mathcal{M}_{11}^N + \mathcal{M}_{12}^N) (\phi^2 R_{N+1} \mathcal{M}_{11}^N + \mathcal{M}_{12}^N)}. \quad (12)$$

A similar expression³ can be derived for segment $n=0$; note that the coefficients \mathcal{M}_{11}^N and \mathcal{M}_{12}^N are known explicitly.

To study the behavior of (12) for $N \rightarrow \infty$, we distinguish two cases.

If τ has nonzero imaginary part, or if τ is real with $|\tau| > 1$, one of the eigenvalues λ_1, λ_2 of \mathcal{M} has norm exceeding one. The N th powers of both eigenvalues occur in (8)–(10), and so \mathcal{M}_{11}^N tends to infinity if N does. Division of the denominator and the numerator of (12) by $(\mathcal{M}_{11}^N)^2$ thus implies $\lim_{N \rightarrow \infty} U_N = 0$.

If τ is real, and $|\tau| \leq 1$, both λ_1 and λ_2 (and their powers) have modulus 1, and are located on the boundary of the complex unit circle. In this case, (12) shows that U_N does not tend to zero for $N \rightarrow \infty$. Combining Eq. (3) for the tool-joint reflection and transmission coefficients with (5), and using the definition of τ , the following resonance condition results:⁴ only sound waves with frequencies for which

$$\text{Im}(\tau) = 0$$

and

$$|\tau| = \left| \cos \kappa \ell \cos \kappa(L - \ell) - \frac{1}{2} \left(\frac{A_j}{A_p} + \frac{A_p}{A_j} \right) \times \sin \kappa \ell \sin \kappa(L - \ell) \right| \leq 1 \quad (13)$$

are able to travel through long drill pipes, all segments and joints of which are identical.

This resonance condition (13), which is also reported in Barnes and Kirkwood (1972) and Drumheller (1989), explains the bandpass filter behavior of the drill pipe visualized in Fig. 5. However, it does not by itself give any information about the fine structure of the frequency response of the pipe's pass bands, which have only been considered numerically by Drumheller (1989) and Barnes and Kirkwood (1972). This fine structure is more apparent in Fig. 6, in which only one pass band is displayed.

Equation (12) gives an analytical expression for this spectrum structure, and allows energy dissipation and pipe segment length variations to be included in the model.

C. Energy dissipation

We model energy dissipation in the drill pipe wall by introducing a linear, dissipative term in the ordinary wave equation:

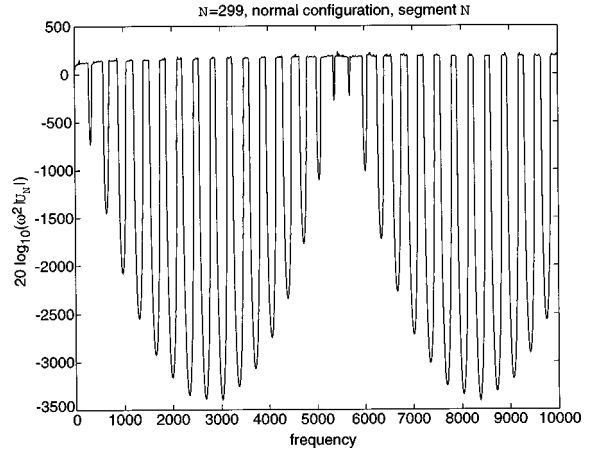


FIG. 5. $20 \log_{10}(\omega^2 |U_N|)$ in the middle of the last segment of a 300-segment drill pipe ($N=299$).

$$\frac{\partial^2 U}{\partial t^2} - c^2 \frac{\partial^2 U}{\partial z^2} = -\beta \frac{\partial U}{\partial t}.$$

Restriction to harmonic solutions as in (2) then gives⁵ $(-\omega^2 + c^2 \kappa_e^2 - i\beta\omega) = 0$, or $\kappa_e^2 = \kappa^2(1 + i\beta/\omega)$. For small dissipative terms β , we may write $\kappa_e = \pm(\kappa + i\alpha)$, with

$$\alpha = \frac{\beta/c}{1 + \sqrt{1 + i\beta/\omega}} \approx \frac{\beta}{2c}.$$

Equation (2) can be rewritten as

$$U(z, t) = (u e^{-\alpha z} e^{i\kappa z} + v e^{\alpha z} e^{-i\kappa z}) e^{-i\omega t},$$

i.e., the sound wave amplitude of sound waves traveling to the left or to the right decreases exponentially with the distance traveled.

Figure 7 shows the consequences of energy dissipation for sound transmission through the drill pipe: the resonance peaks vanish. We have chosen an amplitude attenuation of 10 dB/km, corresponding with $\alpha = 10^{-3}/\log_{10} e$. The configuration consists of 20 pipe segments, connected by $N=19$ tool-joints. Comparing with Fig. 6, we see that in a configu-

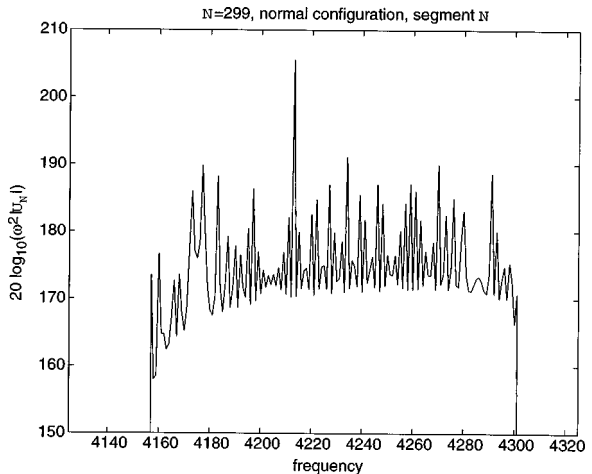


FIG. 6. $20 \log_{10}(\omega^2 |U_N|)$ in the middle of the last segment of a 300-segment drill pipe ($N=299$).

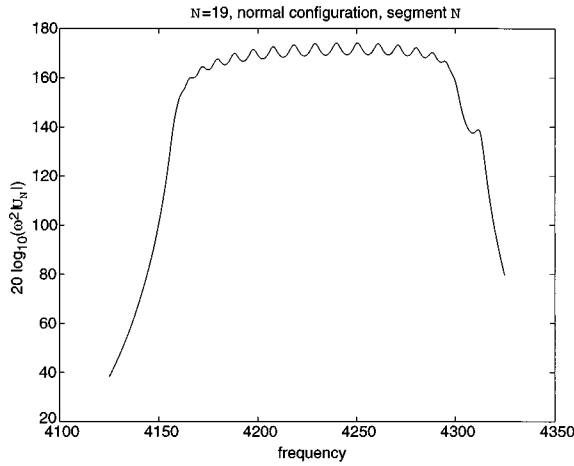


FIG. 7. $20 \log_{10} (\omega^2 |U_N|)$ in the middle of the last segment of a 20-segment drill pipe ($N=19$), with energy dissipation (10 dB/km).

ration with only 19 tool-joints the diffusion has removed the sharp peaks almost completely. This effect becomes even more pronounced for larger values of N .

An alternative way to model the effect of energy losses in the drill pipe is to assume them to occur at the tool-joints only. Instead of introducing a complex wave number κ_e , it then suffices to slightly change the tool-joint reflection and transmission coefficients R and T , such that the determinant Δ of \mathcal{M} becomes smaller than one. Expression (12) remains valid if the second term in its numerator is divided by Δ^N . Furthermore, the eigenvalues λ_1 and λ_2 have to be changed to $\lambda_{1,2} = \tau \pm \sqrt{\tau^2 - \Delta}$ and the conditions $\tau^2 = 1$ and $\tau^2 \neq 1$ have to be modified to $\tau^2 = \Delta$ and $\tau^2 \neq \Delta$ (similarly for inequalities).

D. Pipe segment length variations

To roughly estimate the effect of small pipe segment length variations on the amplitude U_N in the rightmost drill pipe segment, the pipe segment lengths L_n occurring in the phase-shift matrices Φ_n [see (5)] have been disturbed with a normally distributed error l_n with mean zero and standard deviation σ_p .

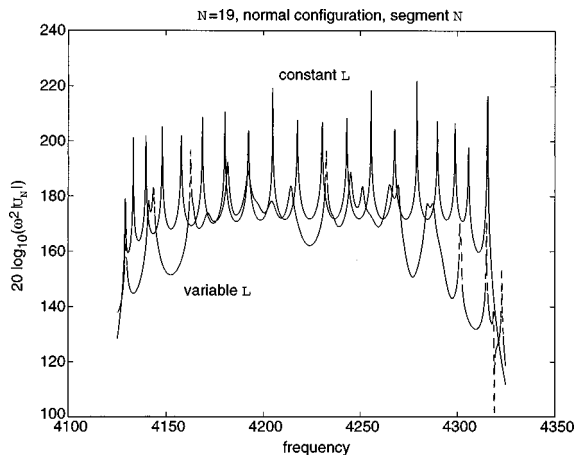


FIG. 8. $20 \log_{10} (\omega^2 |U_N|)$ in the middle of the last segment of a 20-segment drill pipe ($N=19$), with variable pipe segment length ($\sigma_p=0.05$).

The results for a drill pipe with 20 pipe segments and $N=19$ tool-joints are shown in Fig. 8; we have chosen $\sigma_p = 0.05$. The peaks within the pass bands are less sharp compared to those in Fig. 6 (notice that the vertical scales differ in both figures). The stop bands appear to be less pronounced. In fact, the conditions for resonance are never fulfilled exactly if L varies, and neither are the conditions that make different parts of the drill pipe move in exact counter-phase.

Small pipe segment length variations appear to affect mainly the drill pipe's sound transmission properties at higher frequencies. The location of the resonance peaks is slightly affected as well.

III. TIME DOMAIN MODELING

A. Additional simplifications and their motivation

As we want to study sound transmission through the drill pipe in the time domain, we must switch from a stationary situation with harmonic sound waves to a dynamical one, where sound signals are used of which the time duration is limited. We assume them to be so short that they do not interact, i.e., their duration is short compared to the time sound needs to propagate through a pipe segment.⁶ In the sequel, we refer to such short time-duration signals as "pulses" $\hat{u}(t)$.

In order to make sure that the reflection and transmission of a pulse remains pulse shaped, we have to make restrictions on the reflection coefficient $R(\omega)$ at the tool-joints. Assume that an incident signal $u(\omega)$ yields a reflection $v(\omega) = R(\omega)u(\omega)$. After inverse Fourier transformation, this gives the time-domain expression

$$\begin{aligned} \hat{v}(t) &= \int_{-\infty}^{\infty} R(\omega)u(\omega)e^{-i\omega t} d\omega \\ &= \frac{1}{2\pi} \int_{-\infty}^t \hat{R}(t-t')\hat{u}(t')dt', \end{aligned}$$

in which we used causality of $\hat{R}(t)$, the inverse Fourier transform of $R(\omega)$ (Rienstra, 1988). If $\hat{u}(t) = \delta(t)$, this reduces to $\hat{v}(t) = (1/2\pi)\hat{R}(t)$, which is in general not pulselike because $R(\omega)$ is in general not a constant or of the form $\sim e^{i\omega s}$. In fact, substitution of Eq. (3) for $R(\omega)$ yields

$$\begin{aligned} \hat{R}(t) &= -2\pi r_{jp} \delta\left(t + \frac{l}{c}\right) + 2\pi(1 - r_{jp}^2) \\ &\quad \times \sum_{n=1}^{\infty} r_{jp}^{2n-1} \delta\left(t - (2n-1)\frac{l}{c}\right), \end{aligned}$$

i.e., the reflection of a pulse is a pulse train. This calls for further modeling assumptions.

$\hat{R}(t)$ would be pulselike if $(1 - r_{jp}^2)r_{jp} \ll r_{jp}$, or $r_{jp} \approx 1$, an uninteresting trivial case. Alternatively, $\hat{R}(t)$ can be considered pulselike if its energy is concentrated in the first N_0 pulses of the pulse train, such that $(1 - r_{jp}^2)r_{jp}^{2N_0-2}$ is small enough, and the effective duration $N_0 l/c$ of $\hat{R}(t)$ and the corresponding length of the reflected signal $N_0 l$ are short enough.

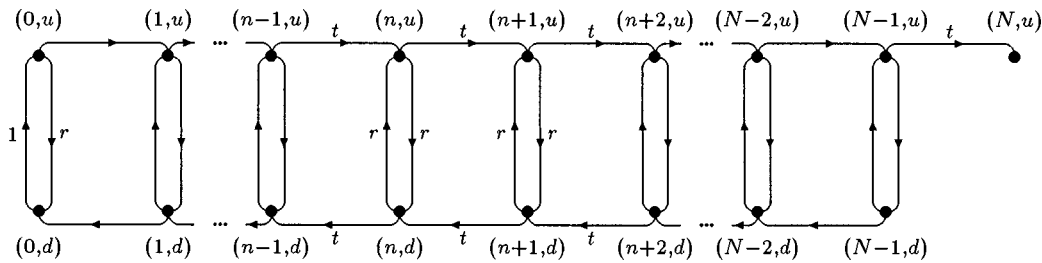


FIG. 9. Drill pipe modeled as a Markov chain.

Implementing these considerations, we assume $R(\omega)$ to be constant in the sequel, and neglect the tool-joint length.

The bandwidth of the sound signals used for data transmission will not exceed the width of the drill pipe's pass bands. According to Eq. (3), the values of R and T generally vary only slightly in such limited spectral intervals. Within the signal's frequency band, it therefore seems realistic indeed to approximate R by a constant.

Furthermore, since $u(\omega)=0$ outside this band, the reflected signal $R(\omega)u(\omega)$ does not change if we assume R to have the same constant value for all ω . By choosing a real value for the reflection coefficient, we neglect phase jumps at reflection.

A similar argument holds for the transmission coefficient T and, at the transducer end, for R_0 . For the sake of demonstration we set $R_0=1$.

Clearly, with respect to the original equation (1), the results presented in the sequel will have to be interpreted as approximations.

B. A Markov model for the drill pipe

Consider an energy pulse of amplitude 1 traveling toward a tool-joint of which the constant reflection and transmission coefficients with respect to energy⁷ are denoted by r and t . At the tool-joint, part of the pulse reflects and part of it is transmitted. Conservation of energy implies

$$1 = r + t.$$

This observation leads to a statistical analogue for (sound) energy pulse propagation through the drill pipe.

We model energy pulses as marbles, rolling from left to right or vice versa within the pipe segments. At each tool-joint, they change direction with probability r . With probability t , they keep rolling in the same direction.

The drill pipe can now be modeled as a Markov chain, introducing two states for each pipe segment.⁸ A "marble" is said to be in state (n, u) if it rolls upward in segment n . If it rolls downward, it is in state (n, d) . The Markov chain is shown in Fig. 9.

Consider one "marble" which starts to roll upward in the first pipe segment at clock unit $k=0$. Let $\pi_k(n, j)$ be the probability that at clock unit k it moves in direction $j \in \{u, d\}$ in pipe segment n . Hence, $\pi_0(0, u)=1$ and for $k=1, 2, \dots$ the probabilities $\pi_k(n, j)$ satisfy (see Fig. 9)

$$\pi_k(0, u) = \pi_{k-1}(0, d), \quad (14)$$

$$\pi_k(n, u) = t\pi_{k-1}(n-1, u) + r\pi_{k-1}(n, d), \quad n=1, \dots, N, \quad (15)$$

$$\pi_k(n, d) = t\pi_{k-1}(n+1, d) + r\pi_{k-1}(n, u), \quad n=0, \dots, N-1, \quad (16)$$

where $\pi_k(N, d)=0$ by definition. From these equations we can easily compute for consecutive values of k the probability distribution $\{\pi_k(n, j)\}$. Figure 10 displays this distribution for some values of k in a configuration with $N=15$ tool-joints (and 16 pipe segments), with $r=0.1$ and $t=0.9$. The value of $\pi_k(N, u)$ for consecutive values of k is shown in Fig. 11; it shows how much energy reaches the upper drill pipe end at each clock unit. We have chosen the same reflection and transmission coefficients, but $N=63$.

In terms of the physical problem, two effects influence the energy pulse propagation. The first will be called **direct transmission**: part of the pulse travels through the drill pipe without reflecting anywhere. This explains the rightmost peak in Fig. 10, for $k=4$ and $k=12$, and the small peak in Fig. 11 at time unit $k=63$. The second effect is similar to **diffusion**. Energy that reflects at a number of tool-joints appears to be distributed more or less regularly throughout the configuration, and diffuses to the upper end of the configuration. This is visible in Fig. 10, for $k=20$ and $k=28$, and explains the "hump" in Fig. 11 following the first peak at $k=63$.

The effect of decreasing t is similar to that of increasing N , and vice versa. For $t=1$, the "hump" disappears: all energy travels through the drill pipe at once. For small values of t , the diffusion effect is large compared to the direct trans-

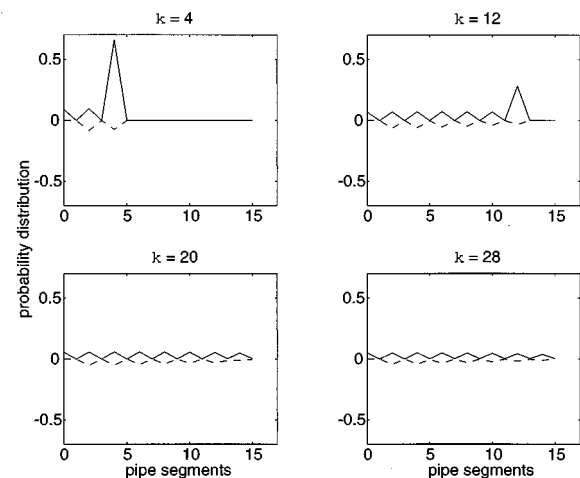


FIG. 10. Probability distribution of the energy pulse ("marble") position after k time units; $N=15$, $r=0.1$, $t=0.9$ (downward probabilities with minus sign).

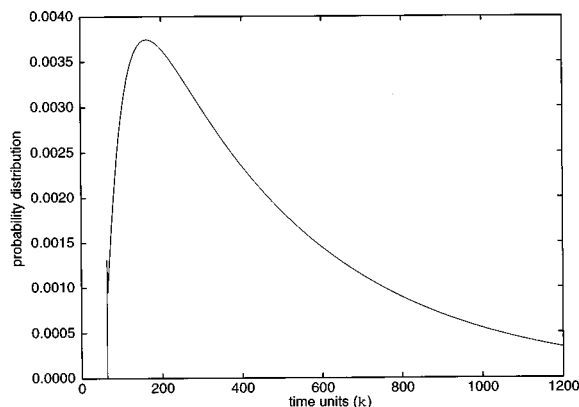


FIG. 11. Probability distribution of the energy pulse (“marble”) arrival after k time units; $N=63$, $r=0.1$, $t=0.9$.

mission, and only the “hump” reaches the upper drill pipe end.

In the following paragraphs, we show that the “hump” is a mixture of N geometric functions. This observation will allow exact determination of the expected traveling time of the energy pulse through an $N+1$ -segment drill pipe. It will also yield an expression for the variance of this traveling time, i.e., an estimate for the width of the “hump.” We will finally show that two geometric functions suffice to closely approximate the shape of the “hump.”

C. The “hump” as a mixture of geometric functions

We introduce the (probability) generating functions

$$F(n, j; z) = \sum_{k=0}^{\infty} \pi_k(n, j) z^k; \quad (17)$$

$F(N, u; z)$ is the generating function of the “hump.” We now show how to determine $F(N, u; z)$ explicitly. This will lead to a mathematical description of the “hump” in terms of geometric functions.

Equations (14)–(16) combined with the initial condition $\pi_0(0, u) = 1$ yield

$$F(0, u; z) = zF(0, d; z) + 1, \quad (18)$$

$$F(n, u; z) = tzF(n-1, u; z) + rzF(n, d; z), \quad n=1, \dots, N, \quad (19)$$

$$F(n, d; z) = tzF(n+1, d; z) + rzF(n, u; z), \quad n=0, \dots, N-1. \quad (20)$$

We rewrite expressions (19) and (20) to

$$\begin{pmatrix} F(n, u; z) \\ F(n, d; z) \end{pmatrix} = \mathcal{W}(z) \begin{pmatrix} F(n-1, u; z) \\ F(n-1, d; z) \end{pmatrix}, \quad n=1, \dots, N, \quad (21)$$

where

$$\mathcal{W}(z) = \begin{pmatrix} (t^2 - r^2)z/t & r/t \\ -r/t & 1/tz \end{pmatrix}. \quad (22)$$

Applying induction to (21), we obtain

$$\begin{pmatrix} F(N, u; z) \\ F(N, d; z) \end{pmatrix} = \mathcal{W}^N(z) \begin{pmatrix} F(1, u; z) \\ F(1, d; z) \end{pmatrix}.$$

We combine this result with (18), and substitute $F(N, d; z) = 0$. This leads to

$$F(N, u; z) = \frac{\det(\mathcal{W}^N(z))}{\mathcal{W}_{22}^N(z) + z\mathcal{W}_{21}^N(z)} = \frac{\det(\mathcal{W}(z))^N}{\mathcal{W}_{22}^N(z) + z\mathcal{W}_{21}^N(z)},$$

in which $\mathcal{W}_{ij}^N(z)$ denotes the ij -component of $\mathcal{W}^N(z)$ for $i, j=1, 2$. Since $\det(\mathcal{W}(z)) = 1$ we eventually find

$$F(N, u; z) = \frac{1}{\mathcal{W}_{22}^N(z) + z\mathcal{W}_{21}^N(z)} =: \frac{1}{f(z)}. \quad (23)$$

As the components of $\mathcal{W}(z)$ are either constants, or multiples of z or $1/z$, it is readily verified that the function $f(z)$ may be written as

$$f(z) = \sum_{k=-N}^N f_k z^k,$$

hence $z^N f(z)$ is a polynomial of degree $2N$.

With Eqs. (17) and (23) we have two different expressions for $F(N, u; z)$, one in terms of the probabilities $\pi_k(N, u)$, the other as the reciprocal of $f(z)$. We now express the probabilities $\pi_k(N, u)$ in terms of the zeros of $z^N f(z)$. These expressions give rise to the mathematical description of the “hump” in Fig. 11 as a mixture of N geometric functions.

To compare (17) and (23), we first exploit some properties of $F(N, u; z)$. Note that it takes at least N clock units for a “marble” to reach pipe segment N and each segment passed in the downward direction must be passed again in the upward direction to ever reach the end of the drill pipe. This implies that $\pi_k(N, u) = 0$ for $k < N$ and $\pi_{N+1+2k}(N, u) = 0$ for $k \geq 0$. Hence

$$F(N, u; z) = z^N \sum_{k=0}^{\infty} \pi_{N+2k}(N, u) z^{2k},$$

from which we can conclude that $F(N, u; z)/z^N$ is even, and convergent for $|z| \leq 1$; it has no poles within the closed unit disk. Thus also $z^N f(z)$ is even. So each zero of $z^N f(z)$ has a companion zero with opposite sign. Furthermore, all zeros of $z^N f(z)$ must be situated outside the closed unit disk. Denote the zeros of $z^N f(z)$ by $z_1, -z_1, \dots, z_N, -z_N$, which we assume to be distinct. We may then write

$$z^N f(z) = f_{-N} (1 - (z/z_1)^2) \cdots (1 - (z/z_N)^2).$$

Partial fraction decomposition of $F(N, u; z)$ now yields

$$\begin{aligned} F(N, u; z) &= \frac{z^N}{z^N f(z)} = \frac{z^N}{f_{-N}} \sum_{i=1}^N \frac{a_i}{1 - (z/z_i)^2} \\ &= z^N \sum_{k=0}^{\infty} z^{2k} \sum_{i=1}^N \frac{a_i}{f_{-N}} \left(\frac{1}{z_i} \right)^{2k}, \end{aligned} \quad (24)$$

with $a_i = 1/\prod_{j=1, j \neq i}^N (1 - z_i/z_j)$. From (17) and (24) we finally get

$$\pi_{N+2k}(N, u) = \sum_{i=1}^N b_i (1 - p_i) p_i^k, \quad k=0, 1, 2, \dots \quad (25)$$

To ease the interpretation of (25), we introduced

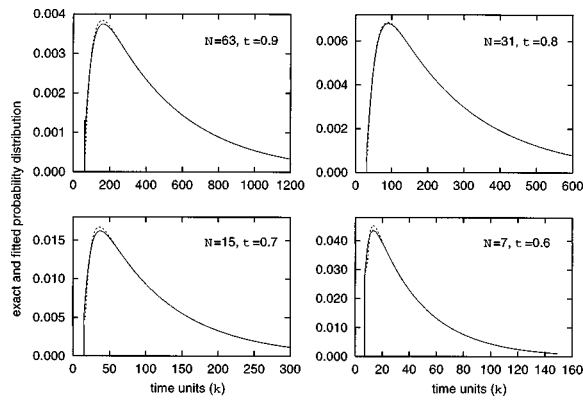


FIG. 12. Expected duration of the energy pulse (“marble’s”) trip through the drill pipe, and its standard deviation as a function of N for various values of t .

$$p_i = 1/z_i^2, \quad b_i = \frac{a_i}{f_{-N}(1-p_i)}, \quad i = 1, \dots, N.$$

It follows that the probabilities $\pi_k(N, u)$ are mixtures of N geometric distributions for $k = N, N+2, \dots$; the “hump” in Fig. 11 is a mixture of N geometric functions.

D. Expectation and variance of an energy pulse’s traveling time

Expression (25) is not useful for practical purposes, since it requires the determination of all zeros of the polynomial $z^N f(z)$. An approximation that appears to be remarkably accurate is obtained by constructing a suitable distribution that fits the mean μ_t and variance σ_t^2 of the time it takes the “marble” to reach the right end of the drill pipe. The distribution that will be used is a discrete version of the continuous K_2 -distribution (Tijms, 1986). Such an approximation, of course, only makes sense if μ_t and σ_t^2 can be easily determined. This is indeed the case. Below we will derive explicit expressions for μ_t and σ_t^2 , by utilizing again the generating function $F(N, u; z)$.

The mean and variance of the traveling time can be found by differentiating the generating function $F(N, u; z)$, yielding⁹

$$\mu_t = \sum_{k=1}^{\infty} k \pi_k(N, u) = F'(N, u; 1) = -\frac{f'(1)}{f^2(1)} = -f'(1),$$

where the prime denotes the derivative with respect to z . For the variance of the traveling time, a similar derivation yields

$$\sigma_t^2 = f'(1)^2 - f''(1) - f'(1).$$

To determine $f'(1)$ and $f''(1)$ note that the format of $\mathcal{W}(z)$ in (22) is extremely similar to that of \mathcal{M} in the frequency domain analysis. The components of $\mathcal{W}^N(z)$ are given by (8)–(10) after proper substitution of the components of $\mathcal{W}(z)$ for the ones of \mathcal{M} . So $f(z)$, and thus also $f'(1)$ and $f''(1)$, can be determined explicitly! After some algebra we find

$$\mu_t = \frac{1}{t} N(1+rN),$$

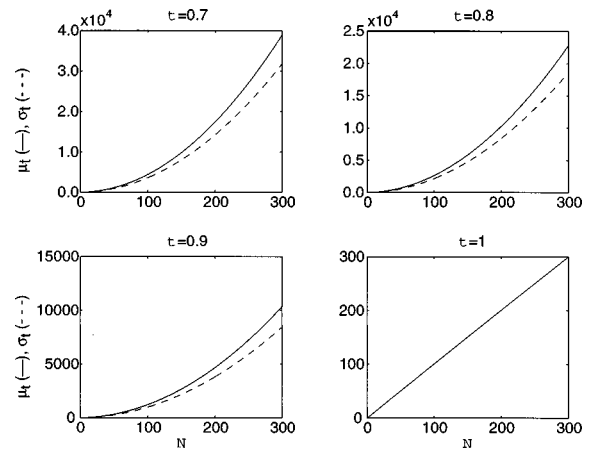


FIG. 13. Fitting of the probability distribution of the energy pulse (“marble”) arrival after k time units for various values of N and t ; exact: —, fitted: ---.

$$\sigma_t^2 = \frac{2r}{3t^2} N(N+1)(1+(1+t)N+rN^2).$$

As could be expected for a diffusionlike process, the time energy pulses need to travel through the drill pipe increases quadratically with N , and so does its standard deviation. Figure 12 displays the results for different transmission coefficients t .

E. Approximation of the “hump” using two geometric functions only

We saw that the “hump,” following the “direct-transmission-peak” at $k=N$, is a mixture of N geometric functions. We now show that, by appropriate parameter choice, only two geometric functions suffice to approximate its shape.

In analogy to Eq. (25), we write

$$\pi_{N+2k}(N, u) = c_1(1-q_1)q_1^k + c_2(1-q_2)q_2^k, \quad k = 1, 2, \dots, \quad (26)$$

thus replacing the N known geometric distributions by two distributions, the parameters of which have to be fitted to the mean and variance of the traveling time of a pulse. Note that the “direct-transmission-peak” is given by

$$\pi_N(N, u) = t^N. \quad (27)$$

The probabilities q_1 and q_2 and the coefficients c_1 and c_2 in (26) are chosen to satisfy

$$q_1 = \frac{a - (1+1/\hat{\mu}) + \sqrt{2a-1/\hat{\mu}}}{a - 1/\hat{\mu}^2 - (1+1/\hat{\mu})^2},$$

$$q_2 = \frac{\hat{\mu} - q_1/(1-q_1)}{1 + \hat{\mu} - q_1/(1-q_1)},$$

$$q_1 c_1 = (1-t^N) - q_2 c_2$$

$$= (1-t^N) \frac{q_1/(1-q_1)}{q_1/(1-q_1) - q_2/(1-q_2)},$$

where¹⁰

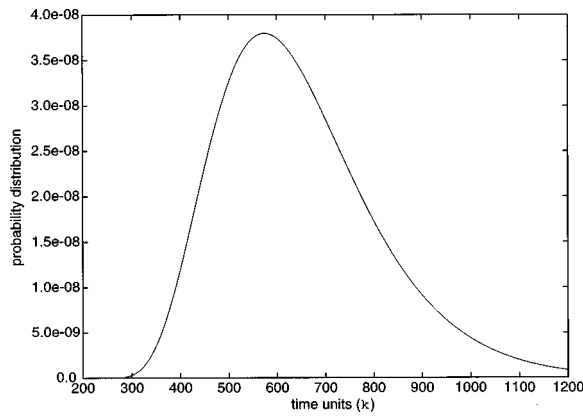


FIG. 14. Probability distribution of the energy pulse (“marble”) arrival after k time units, with energy losses at tool-joints; $N=255$, $r=0.1$, $t=0.9$, $d=0.01$.

$$a = \frac{\hat{\sigma}^2}{\hat{\mu}^2} - \frac{1}{\hat{\mu}}, \quad \hat{\mu} = \frac{1}{2} \left(\frac{\mu_t - Nt^N}{1-t^N} - (N+2) \right),$$

$$\hat{\sigma}^2 = \frac{1}{4} \left(\frac{\sigma_t^2}{1-t^N} - \frac{t^N}{(1-t^N)^2} (\mu_t - N)^2 \right).$$

The resulting distribution, a discrete version of the continuous K_2 -distribution (see Tijms, 1986, pp. 399–400), fits the mean and variance of the traveling time of a pulse, provided $\frac{1}{2} < a < 1$. The fitting result is shown in Fig. 13. Apparently, only two geometrical distributions suffice to provide an excellent description of the “hump.”

The mentioned condition on a holds when N is sufficiently large.¹¹ In case it does not hold, we refer to the recipe described by Adan *et al.* (1995) to find an appropriate discrete distribution to fit the “hump.”

F. Energy dissipation

Energy dissipation in the drill pipe wall can be easily included in the model. Note that $\pi_k(N, u)$ indicates how much energy reaches the upper drill pipe end after k clock units in case there is no energy dissipation. If we assume a fraction d of the energy to dissipate in each clock cycle, the amount of energy reaching the drill pipe end after k clock units is $(1-d)^k \pi_k(N, u)$. This observation is used to obtain the results shown in Fig. 14. Only part of the signal energy reaches the upper drill pipe end. The “hump” therefore becomes less high, but sharper.

IV. CONCLUSIONS

In addition to the results found by Barnes and Kirkwood (1972) and Drumheller (1989), the frequency domain drill pipe model yields explicit expressions for the fine structure of the frequency response within the pass bands, of which the position along the frequency axis is found from a resonance condition as in the work of Barnes and Kirkwood (1972) and Drumheller (1989). After including energy dissipation in the model, the resonance peaks in the pass-bands become less pronounced. Small variations in pipe segment length have the same effect, but also slightly affect the position of these peaks on the frequency axis. The effect of length variations increases with frequency.

In the time domain, the drill pipe can be modeled as a Markov chain, from which expressions result for the expected time a sound signal needs to travel from one side to the other, and its standard deviation. Both increase quadratically with the number of pipe segments. Sound (pulse) propagation through drill pipe and tool-joints is comparable to a diffusion process. Energy pulses input at one end of the drill pipe are received at the other as energy “humps” that become flatter for decreasing transmission coefficient or for increasing drill pipe length. The “humps” appear to be mixtures of geometric functions. For practical purposes, their shape can be approximated well by two geometric functions only, i.e., by a discrete version of the K_2 distribution. Energy dissipation results in less flat, but smaller, output “humps.”

ACKNOWLEDGMENTS

The research leading to this paper was done for, and partly funded by, Hollandse Signaalapparaten (HSA), Hengelo, The Netherlands, under supervision of Emiel Stolp, HSA. The derivation of the wave equation in the drill pipe wall, and the transducer model, are due to Fons van de Ven, TUE.

¹For $|r_{jp}^2 \phi^4| < 1$, T can be written as $t_{pj} t_{jp} \{1 + r_{jp}^2 \phi^4 + r_{jp}^4 \phi^8 + \dots\}$. All sound waves that travel through the tool-joint are attenuated at both discontinuities, and therefore by $t_{pj} t_{jp}$. Waves that make a detour inside the tool-joint, and travel hence and forth once, have a resulting amplitude which is a factor r_{jp}^2 smaller, while their phase has changed by a factor ϕ^2 .

The remaining terms in the power expansion of T have a similar interpretation.

²The factors ϕ introduced to describe the tool-joints have a similar interpretation; we refer to footnote 1.

³The expression for U_N is similar to the one for T in (3). The numerators of both equations represent the effect on a sound wave of traveling through the whole configuration at once. The denominators represent the influence of sound waves that travel up and down the configurations a number of times before leaving them at the rightmost end.

⁴We assume $A_j/A_p + A_p/A_j$ to be smaller than 2. If it equals its upper bound 2, which is the case if $A_j = A_p$, then $|\tau| = |\cos \kappa L| \leq 1$ for all frequencies.

⁵Index e for energy.

⁶Given the pass-band width of some 250 Hz, and the pipe segment length of about 10 m, this assumption is not completely realistic. The Uncertainty Principle (Papoulis, 1984, p. 273) states that the time duration of sound signals with a bandwidth of 250 Hz is lower bounded by $\frac{1}{500} = 0.002$ s; this is just equal to the time L/c sound needs to travel through a pipe segment.

⁷These are different from the amplitude reflection and transmission coefficients!

⁸We assumed complete reflection at the transducer end, and complete absorption at the upper end of the drill pipe.

⁹Note that $f(1) = \mathcal{W}_{22}^N(1) + \mathcal{W}_{21}^N(1) = 1$. In terms of energy pulses, $f(1) = 1$ corresponds to conservation of energy.

¹⁰ $\hat{\mu}$ and $\hat{\sigma}^2$ are the mean and variance of the random variable $\frac{1}{2}(X - (N+2))$, where X is the traveling time a pulse needs to reach the upper end of the drill pipe, given that the traveling time is greater than or equal to $N+2$.

¹¹Using the formulas for μ_t and σ_t^2 it is readily verified that $a \rightarrow \frac{2}{3}$ as $N \rightarrow \infty$. In most cases the condition $\frac{1}{2} < a < 1$ appears to hold for small values of N already.

Adan, I. J. B. F., van Eenige, M. J. A., and Resing, J. A. C. (1995). “Fitting discrete distributions on the first two moments,” *Prob. Eng. Inf. Sci.* **9**, 623–632.

Barnes, T. G., and Kirkwood, B. R. (1972). “Passbands for acoustic transmission in an idealized drill string,” *J. Acoust. Soc. Am.* **51**, 1606–1608.

- Dowling, A. P., and Ffowcs Williams, J. E. (1983) *Sound and Sources of Sound* (Wiley, New York).
- Drumheller, D. S. (1989). "Acoustical properties of drill strings," *J. Acoust. Soc. Am.* **85**, 1048–1064.
- Fletcher, N. H., and Rossing, T. D. (1991). *The Physics of Musical Instruments* (Springer-Verlag, New York).
- Papoulis, A. (1984). *Signal Analysis* (McGraw–Hill, London).
- Rienstra, S. W. (1988). "1-D Reflection at an Impedance Wall," *J. Sound Vib.* **125**, 43–51.
- Tijms, H. C. (1986). *Stochastic Modeling and Analysis: A Computational Approach* (Wiley, New York).
- Timoshenko, S., Young, D. H., and Weaver, W. (1974). *Vibration Problems in Engineering* (Wiley, New York).
- Tropper, A. M. (1969). *Linear Algebra* (Nelson, London).
- van de Ven, A. A. F. (1975). "Interaction of electromagnetic and elastic fields in solids," Ph.D. thesis, Eindhoven University of Technology.